Study of threshold creep behaviour of high-pressure die cast Mg-0.5Nd alloy.

Dr. Sujit Khuntia, Mrutyunjay Parida

Department of Mechanical Engineering, College of Engineering Bhubaneswar

Mail id: khuntiabbsr@gmail.com

Abstract

Under temperatures ranging from 130 to 170 °C and stresses of 30-80 MPa, the threshold creep behavior of high-pressure die-cast Mg-0.5Nd alloy was carefully examined. The investigated alloy had a low activation energy of 102 kJ/mol and a high stress exponent of 8.4. The observed high stress exponent in the alloy under study suggested that the traditional power law had broken down. A threshold stress was added to the analysis for justification, and the high stress exponent was changed to be 5.2. Simultaneously, using the normalization method, a normalized stress exponent of 5 was obtained, taking into account the significant impact of the tested temperature on the minimum creep rate. Both approaches suggested that the dislocation climb was primarily responsible for the creep deformation of the alloy under study. Additionally, TEM observations showed that the origin of the threshold stress may be connected to the Orowan strengthening of dynamically precipitated ultra-thin long -Mg plates in the Mg matrix during creep. The results of the microstructure analysis made it clear that the Mg-0.5Nd alloy's predominant creep mechanism is dislocation climb, though other mechanisms such as reticular eutectic intermetallic phase disintegration, dynamical precipitation of the phase, and twinning also have an impact on this alloy's creep deformation.

1. Introduction

Magnesium (Mg) has a number of benefits that make it a potential candidate for weight reduction in the automotive and aircraft industries, including its high specific strength, low density, effective recyclability, excellent damping capacity, and abundant resources [1-4]. Due to its effective combination of die castability, favorable room-temperature mechanical properties, and adequate corrosion resistance, magnesium alloys, which make up the majority of commercial alloys, have been used successfully in the automotive and electronics industries [2,5-8]. It should be noted that magnesium alloy cannot be used in power train components above 120 °C due to poor creep resistance. Numerous studies have suggested that the $Mg_{17}Al_{12}$ phase's low melting point (437 °C), which is easily made soft and coarse at temperatures above 120 °C, is the main cause of the AZ91 alloy's poor creep resistance [2,9-11]. Up until now, significant efforts have been made to increase the creep resistance of the AZ91 alloy. Microalloying is thought to be the most efficient method for increasing the creep resistance of AZ91 alloy. In addition to reducing the amount of the $Mg_{17}Al_{12}$ phase, addition microalloying elements like Ca [9,10,14], Sr [11,12], rare earth (RE) [10,11], Si [5,15], Bi [15,16], Sb [9,15], and

Sn [16] also introduce thermally stable intermetallic compounds, effectively enhancing the creep properties of the AZ91 alloy.

In order to achieve high creep resistance, alloys like Mg-Al [17], Mg-Zn [18], Mg-Zr [19], and Mg-RE (rare earth) [20] system alloys have been developed. Mg-RE alloys stood out among them due to their exceptional creep resistance, remarkable age-hardening response, and good formability [21]. Specifically, the most prevalent heat-resistant magnesium alloys are Mg-Gd [22], Mg-Y [23], and Mg-Nd [24]. The literature has published a growing amount of research information about Mg-Nd alloy over the past few decades, both experimentally and theoretically. The Mg-2Nd alloy demonstrated good creep resistance due to both solution hardening and, particularly, precipitation hardening, according to Yan et al.'s [25] investigation of the creep behavior of the alloy under a range of temperature and applied stress conditions. According to Hantzsche et al. [26], who thoroughly assessed the impact of Ce, Nd, and Y additions on the microstructure and texture development in Mg-RE alloys, the amount of RE addition necessary for a given element to sufficiently weaken the texture was correlated with the element's solid solubility. In their investigation of the connection between the microstructure and creep resistance in Mg-RE alloys, Zhu et al. [27] concluded that the reinforcement of the -Mg matrix by solid solution and/or precipitation was more significant for the creep resistance of Mg-RE alloys than grain boundary reinforcement by intermetallic phases. When Liu et al. [28] investigated how Al content affected the microstructure and mechanical characteristics of as-cast Mg-5Nd alloys, the results showed that Al additions could significantly lead to the grain refinement of the alloy and that the refined grains and secondary phase strengthening were responsible for the significantly improved mechanical properties. It is well known that microstructures serve as a crucial strategic link between a material's manufacturing process and performance; as a result, further research into the specific interactions between the properties of Mg-Nd alloys' microstructure and microstructure is crucial for controlling the desired microstructure and enhancing performance.

Additionally, some recent studies [29–31] showed that the formation of fine precipitates of metastable phases was the cause of the Mg–Nd alloy's high strength and good creep resistance. High-angle annular detector dark-field scanning transmission electron microscopy was used by Saito et al. [32] to examine the microstructure of precipitates formed in a Mg-0.5Nd alloy. The results suggested that the precipitation sequence could be Mg-solution→GP-zone→Mg7Nd (orthorhombic)→Mg3Nd (FCC). To study the heterogeneous nucleation of b1 precipitates in Mg-0.5 at.% Nd alloy, Liu et al. [33] created a phase-field model. The authors discovered that b1 precipitated as ultra-thin laths with abnormally high aspect ratios under the influence of a screw dislocation's stress field. There is still a dearth of thorough research on the creep behavior of Mg-0.5Nd alloy, which was the goal of the current work. Therefore, in order to encourage the use of Mg-0.5Nd alloy in automotive power components in the future, a thorough investigation of creep mechanism must be provided. In the current study, the creep behavior of a high-pressure die-cast Mg-0.5Nd alloy under stresses of 30-80 MPa and 130-170 °C is thoroughly examined. On the basis of analyses of the stress exponent and activation energy, as well as microstructural observations, the dominant creep mechanism in the studied alloy is discussed.

2. Experimental Procedure

Under the protection of a shield gas made up of CO2 + 2 vol% SF6, pure magnesium and master alloys containing 15 weight percent Nd were melted in a steel crucible at 720 5 °C. The melt was then kept static for 30 minutes and cooled to 710 5 °C after being held for 20 minutes and fully stirred for 10 minutes. A 350 t clamping force cold chamber die-cast machine was used to complete the die-casting process. The result was some die-cast plates with dimensions of 200 mm in length, 80 mm in width, and 2 mm in thickness. By using inductively coupled plasma atomic emission spectroscopy, the actual chemical compositions of the experimental alloy were found to be Mg-0.82Nd in mass percent. From the die-cast plates, creep specimens with dimensions of 25mm gauge length, 6mm width, and 2mm thickness were created. At 130–170 °C, a constant load tensile creep test was conducted with an applied stress of 30–80 MPa. When the temperature reaches the target temperature for each creep test, it is maintained for 10 minutes before loading. The total creep strain was measured using a displacement transducer installed in the creep testing machine. The creep time-strain curves were used to calculate the minimum creep rate. In order to investigate the stress exponent, the creep time-strain curves obtained at 150 °C and 40–80 MPa were used, while those obtained at 70 MPa and 130–170 °C were used to calculate the creep activation energy. Once the minimum creep rate was reached, the majority of tests were stopped.

A FEI-XL30 field emission scanning electron microscope (SEM) and a Philips CM20 transmission electron microscope (TEM) were used to examine the microstructure. The mechanical polishing method was used to prepare the samples for the SEM observations, which was followed by etching. The 3mm diameter, 40 m thick discs that served as the TEM samples were punched. With the aid of a low-energy ion beam and a liquid nitrogen cooling system, these foils were further thinned (milling parameters: Ar, 4 kV, 120 min).

3. Results

3.1. Creep Behaviour

The Mg-0.5Nd alloy's representative creep strain-time curves at 150 °C and 40-80 MPa and 130-170 °C and 70 MPa, respectively, are shown in Figs. 1a and b. It appears that the creep behavior was significantly influenced by both the applied stress and temperature. For instance, when crept at 150 °C and 40-60 MPa, the primary stage and steady state stage were observed, but the tertiary stage was absent. However, when the applied stress was increased to 70 MPa, the creep rate clearly increased and the tertiary stage was clearly visible in the creep curve. Furthermore, a clearly defined steady state was seen, but due to sudden failure, the tertiary creep stage could not be seen when creeping at 150 °C and 70 MPa or 170 °C and 70 MPa. This suggests that the die-cast Mg-0.5Nd microstructure is unstable and experienced notable variation during creep [34]. Die-cast Mg-3Al-1Si (AS31) alloy was also found to exhibit a similar phenomenon [34]. Typically, the creep behavior is described by the traditional power law relationship [2,11,34,35], where Q is the activation energy for the creep, R is the gas constant (8.314 kJ/molK), T is the test temperature (absolute temperature), A is a material-related constant, is the applied stress, n is the stress exponent, and is the minimum creep rate. In Fig. 2a, plots of the Mg-0.5Nd alloy's minimum creep rate versus applied stress are shown using double logarithmic coordinates. The stress exponent of the Mg-0.5Nd alloy, which is slightly higher than those of corresponding from most

Therefore, in order to fully comprehend the creep behavior of the Mg-0.5Nd alloy, it is necessary to investigate the dominated creep mechanisms in depth.

creep mechanisms, was confirmed as 8.4 by measuring the slope of the plots. Additionally, as shown in Fig. 2b, the Arrhenius plots of the minimum creep rate's logarithm against the temperature's reciprocal in the given temperature range produced creep activation energy. The calculated stress-dependent activation energy Q, which is approximately 102 kJ/mol, is slightly higher than the activation energy for magnesium pipe diffusion (92 kJ/mol), but significantly lower than the activation energies for

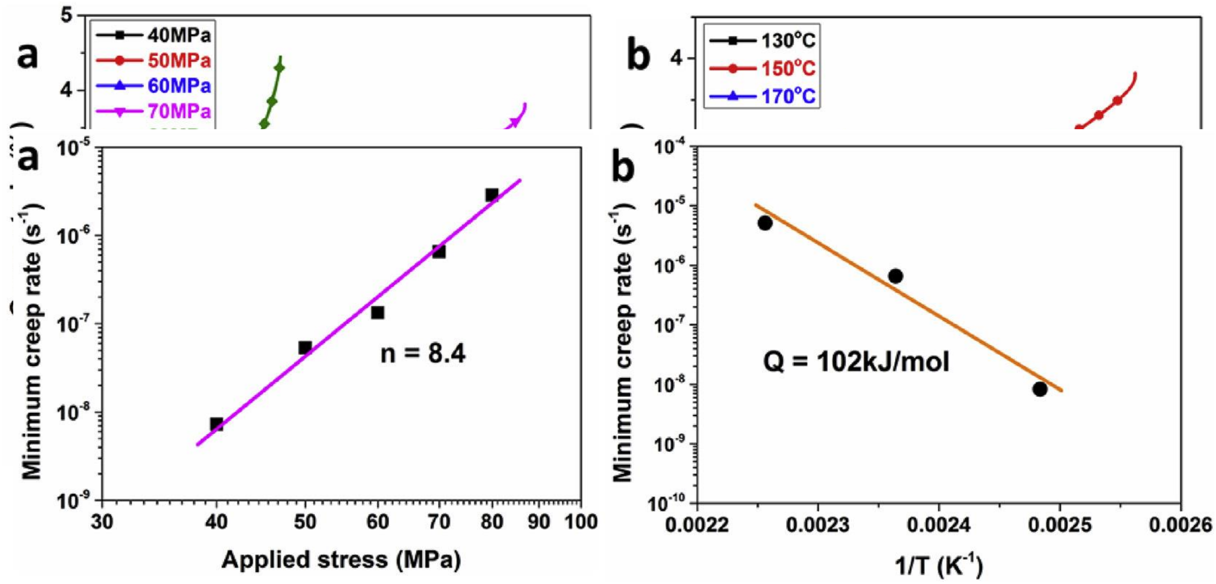

magnesium lattice self-diffusion (135 kJ/mol) [2,7,11,35]. Fig 1: The representative creep strain-time curves of die cast Mg-0.5Nd alloy under (a) 150 °C, 40–80 MPa and (b) 70 MPa, 130–170 °C.

Fig 2: (a) Minimum creep rate plotted against applied stress and (b) temperature dependence on minimum creep rate for die cast Mg-0.5Nd alloy.

3.2. Microstructure Evolution

The typical die-cast microstructure of the Mg-0.5Nd alloy is shown in Figs. 3a and b.

It displays the morphology and distribution of β1 precipitate in the Mg-0.5Nd alloy that was heated for 10 hours at 250°C to reach peak-aged condition. The [0001] direction is where the picture was taken. The β1 precipitate microstructure shown in Fig. 3a is typical, and the β1 particles appear to have precipitated uniformly within the α-Mg matrix. The spatial distribution of β1 precipitates in the area designated A in Fig. 3b is the same as it was in Fig. 3a. However, the distributions of β1 precipitates in the other regions designated as B, C, and D are obviously different from those in region A. The β1 precipitates in region B have an abnormally large aspect ratio, the β1 precipitates in region C form a closely correlated array, and the 1 precipitates in region D form a zigzag structure. Since the interactions between β1 particles alone cannot account for all of the aforementioned abnormal microstructures in regions B, C, and D, they may be linked to pre-existing linear defects. Amberger et al. [36] noted that β1 is roughly 3–4 times harder than α-Mg, which is consistent with β1 being resistant to plastic deformation [36,38]. Dislocation slipping typically happened during creep deformation, piling up a lot of dislocation on the β1 and creating a lot of stress concentration. This happened in the α-Mg grain interior.

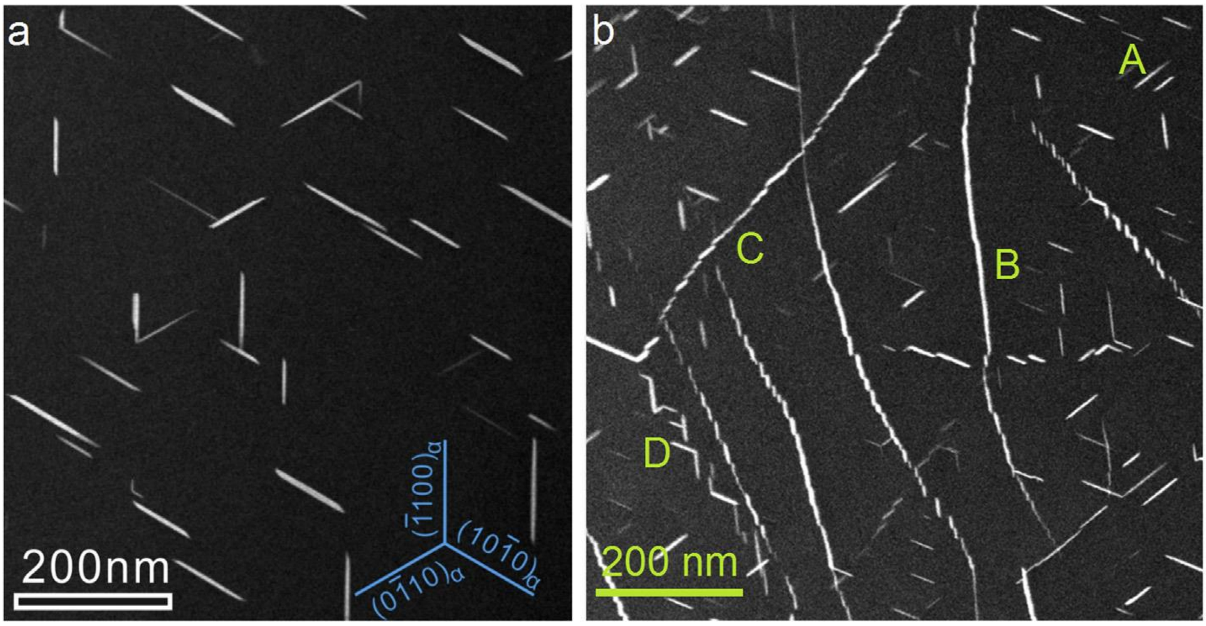

Fig 3: HAADF-STEM images showing b1 precipitates in an Mg-0.5Nd alloy. Electron beam is parallel to $[0001]_\alpha$. Precipitates in (a) form homogeneously, while precipitates in regions B, C and D in (b) form heterogeneously on certain pre-existing linear defects.

FIB-SEM analyses were carried out, as depicted in Figure 4, to more clearly observe the precipitate development in Mg-0.5Nd system alloys. A good contrast between intermetallic or eutectic phases and the α-Mg matrix can be seen in SEM images. Utilizing the contrast between the various phases in the microstructure, different grayscale images were obtained, from which the intermetallic or eutectic phases and α -Mg matrix were identified. Figures 4a and 4b show that the Mg-0.5Nd alloy is primarily made up of the phases α-Mg and a secondary phase (β phase, $Mg_{12}Nd$). The oversaturation of the non-equilibrium solidification of Nd in α-Mg causes some of the Nd to form divorced eutectic β-$Mg_{12}Nd$ instead of precipitating in the as-cast alloys, resulting in the formation of a secondary phase.

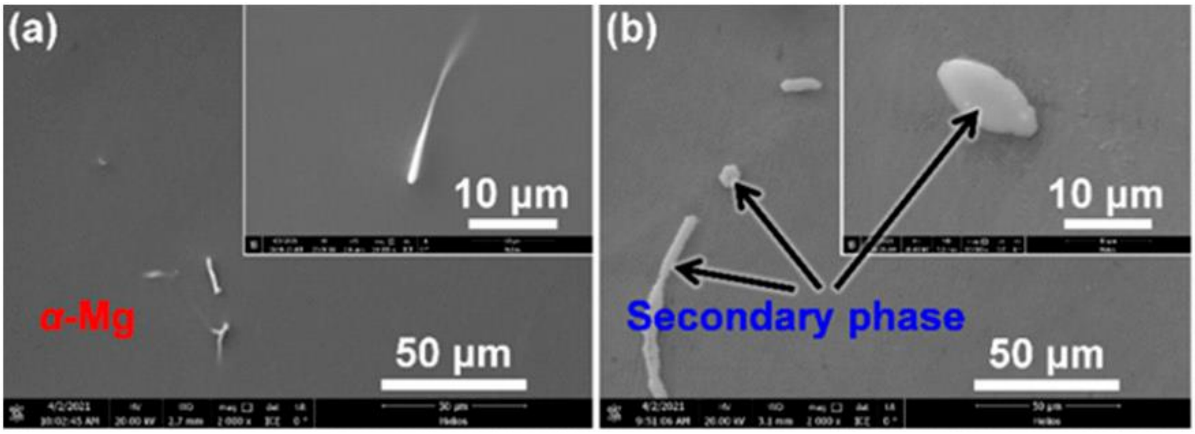

Fig 4: 4. Low- and high-magnification SEM images of precipitates in Mg-0.5Nd Alloy.

4. Discussion

The measured stress exponent is typically used to evaluate the primary creep mechanism. Diffusional creep is associated with n=1 in magnesium alloys, grain boundary slipping is associated with n=2, and dislocation climb is typically associated with n=3–7, but n > 7 indicates power law breakdown [2]. In this study, the Mg-0.5Nd alloy has a higher n value than the typical die-cast Mg alloy [11]. However, many Mg alloys have also been reported to have high n values (n > 7) [34,35]. Such instances, where the interaction between the dislocations and hardened particles during creep can result in a power law breakdown, have been seen frequently in precipitate and/or dispersion hardened alloys [34,35]. In order to explain those high stress exponents, it is frequently adapted to analyze the creep behavior of particle-hardened or die-cast alloys by introducing the threshold stress. Since there is no discernible creep strain, the threshold stress (σ_0) is regarded as a lower ultimate stress. In die-cast AE44 alloy, Zhu et al. [41] reported abnormally high stress exponent values of 41–67. These anomalous stress exponents were changed to be 3-10 after applying the threshold stress method. A modified power law relationship called Garofalo's sinh relationship was used to rationalize the high stress exponents of 9.5-

14.4 that the die-cast AS31 alloy displayed at 125–175 °C to 5 [34]. In reality, these die-cast magnesium alloys can be thought of as composite materials because in the grain boundary regions, soft α-Mg cores were encased in hard intermetallic shells. Therefore, in those die-cast alloys, the widely used threshold stress method was applied. According to a method Li et al. [34] proposed, the threshold stress for creep deformation can be calculated from the plot of $\in^{1/n}$ against applied stress when $\in^{1/n}$ is extrapolated to zero. Analysis typically used n values of 3, 5, 7, and 8, where n stands for the viscous glide process, core diffusion-controlled dislocation climb at low temperatures, lattice self-diffusion-controlled dislocation climb at high temperatures, and a constant structure model controlled by lattice self-diffusion, respectively [13,34,35]. These fitting plots for n=3, 5, 7, and 8 are shown in Fig. 8, where for n=3, 5, and 8, there is no adaptive linear fit between $\in^{1/n}$ and the applied stress, but there is an ideal linear fit for n=7. By assuming n=7, the threshold stress was therefore calculated to be 20 MPa, and was then added to Eq. (2) to normalize the high stress exponent. The minimum creep rate is plotted against the effective stress $(\sigma - \sigma_0)$ in Figure 9. The modified stress exponent was found to be 5.2, which is close to 5 and suggests that the Mg-0.5Nd alloy may be susceptible to dislocation climb. This outcome shows excellent agreement with the findings of the microstructure analysis.

As was already mentioned, precipitation- and/or dispersion-hardened alloys frequently experienced such cases of high stress exponent. Quantities of precipitates formed during creep in the Mg matrix. It is therefore undeniable that these β precipitates dynamically

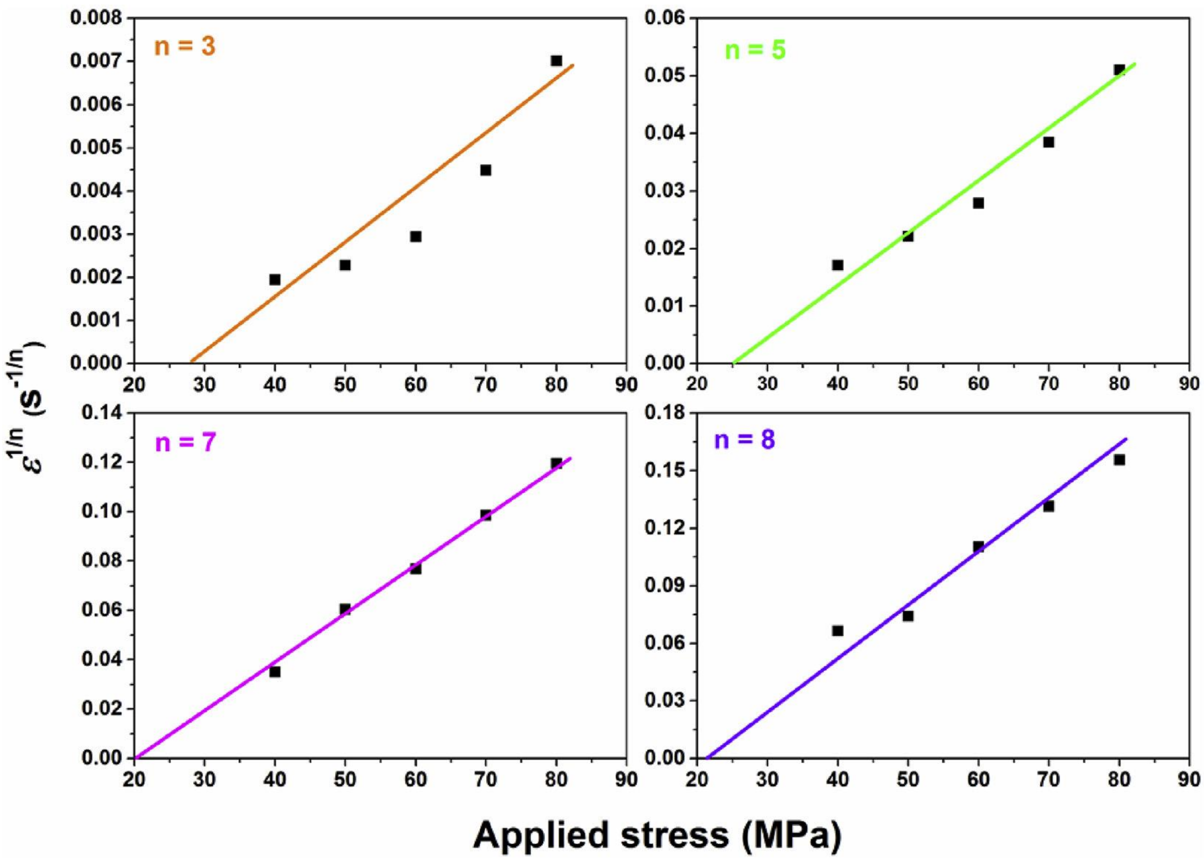

Fig 8: Minimum creep rate plotted as $\varepsilon^{1/n}$ against applied stress for n values of 3, 5, 7 and 8 for die cast Mg-0.5Nd alloy at 150 °C. The best linear relationship seems to be obtained for n=7, where the threshold stress was measured to be approximate 20 MPa.

interacted with dislocations during creep, the Orowan strengthening effect is created [13,17], which may be a significant factor in the threshold stress in the alloy under study. As a result, the threshold stress derived from the creep data and the Orowan stress were calculated to be approximately 24 MPa. We can therefore reasonably conclude that the power law breakdown is caused by the Orowan strengthening, which causes a threshold stress. Additionally, Kunst et al. [17] showed that the Orowan stress induced by Al-Mn particles can be primarily attributed to the threshold stress of the AJ62 alloy, which strongly suggests that this particle strengthening effect results in a higher stress exponent. On the other hand, taking into

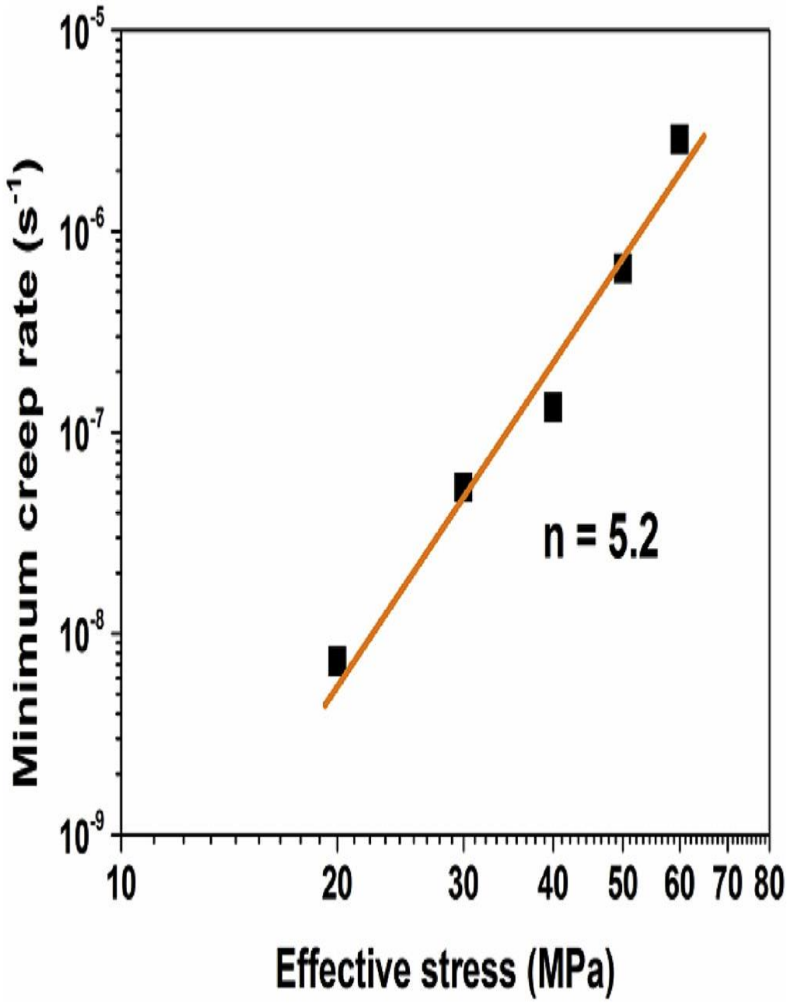

Fig. 9. Minimum strain rate vs. effective stress for die cast Mg-0.5Nd alloy.

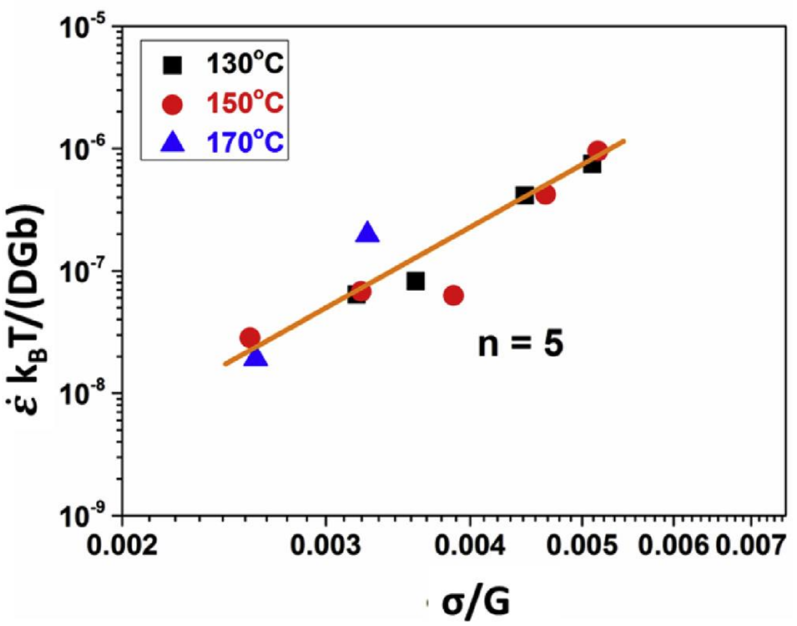

Fig. 10: Relationship between normalized minimum creep rate and normalized stress for die cast Mg-0.5Nd alloy.

account the strong influence of the temperature on the creep rate, the minimum creep rate was normalized as $\dot{\varepsilon} k_B T/(DGb)$ and the stress as σ/G, with a Boltzmann constant kB, self-diffusion coefficient $D=D_0\times\exp[-Q_s/(RT)]$ with $D_0=1\times10{-}4$ m^2s^{-1}, $Q_s=135$ kJ/mol, shear modulus of $G=16.6\times[1-5.3\times10^{-4}((T/K)-300)]$ GPa, and magnitude of the (<a>-type) Burgers vector of $b=3.2\times10^{-10}$ m, where all values were obtained from Refers [13,17,36]. The correlation between $\dot{\varepsilon} k_B T/(DGb)$ and σ/G for the present Mg-0.5Nd alloy is illustrated in Fig. 10. The Mg-0.5Nd alloy's creep deformation was controlled by dislocation climb, and this is further supported by the finding that a normalized stress exponent of 5 was obtained. In conclusion, dislocation climb was determined to be the predominant creep mechanism in the studied alloy based on the analysis of the stress exponent above, which strongly agreed with the conclusions drawn from the analysis of the crept microstructure. The reticular eutectic phases, dynamical platelets, and twinning all disintegrated, according to the aforementioned microstructural observations, aiding in the creep deformation of the Mg-0.5Nd alloy.

5. Conclusions

Under temperatures ranging from 130 to 170 °C and stresses of 30-80 MPa, the creep behavior of high-pressure die-cast Mg-0.5Nd alloy was carefully examined. First, 8.4 and 102 kJ/mol, respectively, were calculated as the stress exponent and activation energy based on the conventional power law relationship. A threshold stress was then added to the analysis, changing the stress exponent to 5.2. In addition, taking into account the significant impact of temperature on creep rate, a normalized stress exponent of 5 was obtained by applying the normalization method. Both imply that dislocation climb was responsible for the studied alloy's creep deformation. Last but not least, the TEM observation showed that extra platelets precipitated in the Mg matrix, resulting in the Orowan strengthening effect, which in turn caused the threshold stress. The disintegration of the reticular eutectic phase disintegration, dynamical precipitation of, and twinning also contributed to the creep deformation of the Mg-0.5Nd alloy, which was further supported by the microstructure analysis. The conventional power law relationship should be used with caution when analyzing the stress exponents of Mg alloys in creep, especially for die-cast alloys, it is suggested. Finally, the findings of this study provide insight into the creation of a die-cast magnesium alloy that is creep-resistant at high temperatures.

References

1) F. Meng, S. Lv, Q. Yang, P. Qin, J. Zhang, K. Guan, Y. Huang, N. Hort, B. Li, X. Liu, J. Meng, Developing a die casting magnesium alloy with excellent mechanical performance by controlling intermetallic phase, J. Alloy. Comp. 795 (2019) 436–445.
2) A.A. Luo, Recent magnesium alloy development for elevated temperature applications, Int. Mater. Rev. 49 (2004) 13–40.
3) K. Guan, F. Meng, P. Qin, Q. Yang, D. Zhang, B. Li, W. Sun, S. Lv, Y. Huang, N. Hort, J. Meng, Effects of samarium content on microstructure and mechanical properties of Mg–0.5Zn–0.5Zr alloy, J. Mater. Sci. Technol. 35 (2019) 1368–1377.
4) D. Zhang, Q. Yang, K. Guan, B. Li, N. Wang, P. Qin, B. Jiang, C. Sun, X. Qin, Z. Tian, Z. Cao, J. Meng, A high-strength low-rare-earth-alloyed magnesium alloy via traditional hot-extrusion, J. Alloy. Comp. 810 (2019) 151967.
5) W. Blum, P. Zhang, B. Watzinger, B.v. Grossmann, H.G. Haldenwanger, Comparative study of creep of the die-cast Mg-alloys AZ91, AS21, AS41, AM60 and AE42, Mater. Sci. Eng. A 319–321 (2001) 735–740.
6) F. Khomamizadeh, B. Nami, S. Khoshkhooei, Effect of rare-earth element additions on high-temperature mechanical properties of AZ91 magnesium alloy, Metall. Mater. Trans. A 36 (2005) 3489–3494.
7) S. Spigarelli, Creep of a thixoformed and heat treated AZ91 Mg-Al-Zn alloy, Scr. Mater. 42 (2000) 397–402.
8) B. Zhang, C. Yang, Y. Sun, X. Li, F. Liu, The microstructure, mechanical properties and tensile deformation mechanism of rolled AlN/AZ91 composite sheets, Mater. Sci. Eng. A 763 (2019) 138118.
9) S. Ganguly, A.K. Mondal, Influence of SiC nanoparticles addition on microstructure and creep behavior of squeeze-cast AZ91-Ca-Sb magnesium alloy, Mater. Sci. Eng. A 718 (2018) 377–389.
10) B. Nami, H. Razavi, S. Mirdamadi, S.G. Shabestari, S.M. Miresmaeili, Effect of Ca and rare earth elements on impression creep properties of AZ91 magnesium alloy, Metall. Mater. Trans. A 41 (2010) 1973–1982.
11) D. Zhang, D. Zhang, F. Bu, X. Li, K. Guan, Q. Yang, S. Liu, X. Liu, J. Meng, Effects of minor Sr addition on the microstructure, mechanical properties and creep behavior of high pressure die casting AZ91-0.5RE based alloy, Mater. Sci. Eng. A 693 (2017) 51–59.
12) G. Cao, C. Zhang, H. Cao, Y.A. Chang, S. Kou, Hot-tearing susceptibility of

ternary Mg-Al-Sr alloy castings, Metall. Mater. Trans. A 41 (2010) 706–716.

13) P. Zhang, Creep behavior of the die-cast Mg–Al alloy AS21, Scr. Mater. 52 (2005) 277–282.
14) J. Majhia, A.K. Mondal, Microstructure and impression creep characteristics of squeeze-cast AZ91 magnesium alloy containing Ca and/or Bi, Mater. Sci. Eng. A 744 (2019) 691–703.
15) A. Srinivasan, J. Swaminathan, U.T.S. Pillai, K. Guguloth, B.C. Pai, Effect of combined addition of Si and Sb on the microstructure and creep properties of AZ91 magnesium alloy, Mater. Sci. Eng. A 485 (2008) 86–91.
16) R. Mahmudi, S. Moeendarbari, Effects of Sn additions on the microstructure and impression creep behavior of AZ91 magnesium alloy, Mater. Sci. Eng. A 566 (2013) 30–39.
17) S. Li, W. Zheng, B. Tang, D. Zeng, X. Guo, Grain Coarsening Behavior of Mg-Al Alloys with Mischmetal Addition, J. Rare Earths 25 (2007) 227–232.
18) Y. Kojima, T. Aizawa, S. Kamado, Mechanical Properties of Rapidly Solidified Mg-Zn Alloys, Mater. Sci. Forum 350–351 (2000) 105–110.
19) R-L. Niu, F.J. Yan, Y.-S. Wang, D.-P. Duan, X.-M. Yang, Effect of Zr content on damping property of Mg–Zr binary alloys, Mater. Sci. Eng. A 718 (2018) 418–426.
20) H. Guo, S. Liu, L. Huang, D. Wang, Y. Du, M. Chu, Thermal Conductivity of As-Cast and Annealed Mg-RE Binary Alloys, Metals 11 (2021) 554.
21) D. Liu, D. Yang, X. Li, S. Hu, Mechanical properties, corrosion resistance and biocompatibilities of degradable Mg-RE alloys: A review, J. Mater. Res. Technol. 8 (2018) 1538–1549.
22) L. Yang, Y. Yuan, T. Chen, X. Dai, L. Zhang, A. Tang, W. Yi, L. Zhang, F. Pan, Diffusion behaviour and mechanical properties of binary Mg–Gd system, Intermetallics 133 (2021) 107171.
23) A. Sudholz, K. Gusieva, X.-B. Chen, B. Muddle, M. Gibson, N. Birbilis, Electrochemical behaviour and corrosion of Mg–Y alloys, Corros. Sci. 53 (2011) 2277–2282.
24) Y. Zhang, Y. Huang, F. Feyerabend, C. Blawert, W. Gan, E. Maawad, S. You, S. Gavras, N. Scharnagl, J. Bode, Influence of the amount of intermetallics on the degradation of Mg-Nd alloys under physiological conditions, Acta Biomater. 121 (2021) 695–712.
25) J. Yan, Y. Sun, F. Xue, S. Xue, W. Tao, Microstructure and mechanical properties in cast magnesium–neodymium binary alloys, Mater. Sci. Eng. A 476 (2008) 366–371.
26) K. Hantzsche, J. Bohlen, J. Wendt, K.U. Kainer, S.B. Yi, D. Letzig, Effect of rare earth additions on microstructure and texture development of magnesium alloy sheets, Scr. Mater. 63 (2010) 725–730.
27) S. Zhu, M. Gibson, M. Easton, J. Nie, The relationship between microstructure and creep resistance in die-cast magnesium–rare earth alloys, Scr. Mater. 63 (2010) 698–703.
28) D. Liu, J. Song, B. Jiang, Y. Zeng, Q. Wang, Z. Jiang, B. Liu, G. Huang, F. Pan, Effect of Al content on microstructure and mechanical properties of as-cast Mg-5Nd alloys, J. Alloy. Compd. 737 (2017) 263–270.
29) Z. Xu, M. Weyland, J. Nie, On the strain accommodation of β precipitates in magnesium alloy WE54, Acta Mater. 75 (2014) 122–133.

30) S. DeWitt, E.L.S. Solomon, A.R. Natarajan, V. Araullo-Peters, S. Rudraraju, L.K. Aagesen, B. Puchala, E.A. Marquis, A.V.D. Ven, K. Thornton, Misfit-driven 0 0 0 precipitate composition and morphology in Mg-Nd alloys, Acta Mater.136 (2017) 378–389.

31) B. Sun, J. Tan, H. Zhang, Y. Sun, Atomic scale investigation of a novel metastable structure in aged Mg–Nd alloys, Scr. Mater. 161 (2018) 6–12.

32) K. Saito, K. Hiraga, The Structures of Precipitates in an Mg-0.5 at% Nd Age-Hardened Alloy Studied by HAADF-STEM Technique, Mater. Trans. 52 (2011) 1860–1867.

33) H. Liu, Y. Gao, Y. Zhu, Y. Wang, J. Nie, A simulation study of β precipitation on dislocations in an Mg–rare earth alloy, Acta Mater. 77 (2014) 133–150.

34) S.M. Zhu, M.A. Easton, M.A. Gibson, M.S. Dargusch, J.F. Nie, Analysis of the creep behavior of die-cast Mg–3Al–1Si alloy, Mater. Sci. Eng. A 578 (2013) 377–382.

35) Q. Yang, X. Qiu, S. Lv, F. Meng, K. Guan, B. Li, D. Zhang, Y. Zhang, X. Liu, J. Meng, Deteriorated tensile creep resistance of a high-pressure die-cast Mg–4Al–4RE–0.3Mn alloy induced by substituting part RE with Ca, Mater. Sci. Eng. A 716 (2018) 120–128.

36) D. Amberger, P. Eisenlohr, Mathias Goken, On the importance of a connected hardphase skeleton for the creep resistance of Mg alloys, Acta Mater. 60 (2012) 2277–2289.

37) W. Blum, Y.J. Li, X.H. Zeng, P. Zhang, B. von Großmann, C. Haberling, Creep deformation mechanisms in high-pressure die-cast magnesium–aluminum–base alloys, Metall. Mater. Trans. A 36 (2005) 1721–1728.

38) W. Blum, B. Watzinger, P. Zhang, Creep of die-cast light-weight Mg–Al-base alloy AZ91hp, Adv. Eng. Mater. 2 (2000) 349–355.

39) J.R. Terbush, A. Suzuki, N.D. Saddock, J.W. Jones, T.M. Pollock, Dislocation substructures of three die-cast Mg–Al–Ca–based alloys, Scr. Mater. 58 (2008) 914–917.

40) Y. Liu, D. Zhao, X. Nie, H. Tao, J. Wang, J. Gui, In situ transmission electron microscopy observations of precipitation and a new orientation relationship between γ-Mg17Al12 and magnesium-based matrix in an Mg–Al–Zn–Sn alloy, Philos. Mag. Lett. 92 (2012) 668–674.

41) S.M. Zhu, M.A. Gibson, J.F. Nie, M.A. Easton, T.B. Abbott, Microstructural analysis of the creep resistance of die-cast Mg–4Al–2RE alloy, Scr. Mater. 58 (2008) 477–480.